Supplemental Appendix

Material and Methods

Patients and samples

Included into this study were n=113 patients with diagnosed *BCR::ABL1*-positive B cell precursor acute lymphoblastic leukemia (BCP-ALL; GMALL cohort). Patients were diagnosed between 2006 and 2021 (analyzed for outcome: 2014-2021) and treated according to the German Multicenter Study Group for Adult Acute Lymphoblastic Leukemia (GMALL) 2008 clinical trial or GMALL registry protocol (NCT02872987, NCT02881086). The GMALL studies were approved by the ethical committees of the participating centers and patients gave written informed consent for biological research. Diagnostic flow cytometry was performed in the central reference laboratory of the study group. Analysis of *BCR::ABL1* minimal residual disease (MRD) was performed in routine diagnostics as previously described.[1] Clinical outcome data were collected by the GMALL study center, Frankfurt. Written informed consent was obtained from patients. All samples were enriched for mononuclear cells by Ficoll density gradient centrifugation prior to RNA extraction or cell sorting.

Transcriptomic sequencing

High-quality RNA samples were submitted for sequencing. Sequencing libraries were prepared using the TrueSeq RNA Library Kit from Illumina according to manufacturer's protocol. Libraries were sequenced 100 base pairs paired-end using the NovaSeq 6000 next generation sequencing platform (Illumina, San Diego, CA, USA) to attain 30 million reads per sample. The obtained reads were aligned to the hg38 reference genome using STAR2.7.1a.

Unsupervised cluster identification in *BCR::ABL1*-positive BCP-ALL samples

We applied an unsupervised approach for grouping of n=113 GMALL samples, which represented the largest cohort, using genes selected by dip test and combination of multiple combination of Uniform Manifold Approximation and Projection (UMAP) analyses.[2] The selection of genes from high-dimensional RNA-Seq data determines the unsupervised grouping of samples and a comparison of 13 feature selection methods showed that dip

performed best to identify cancer subtypes.[3] Thus, we removed genes correlating to patient's sex (abs(ρ>=0.2)) and used Hartigans' dip test that is a test for multimodality (implemented in the R package "diptest") and selected 200 genes with lowest p-value. For grouping of samples, we used UMAP (implemented in the R package "umap") which results are mainly dependent on two settings i.e., nearest neighbors and minimal distance. For averaging UMAP results we combined different parameters for n_neighbors = 3, 5, 10, 20 and 80 with min_dist = 0.0125, 0.05, 0.1, 0.2, 0.5 and 0.8. Distances between samples in the UMAP were z-transformed and averaged across the 30 setting combinations (**Supplemental Figure 1**). Final groups were assigned by hierarchical clustering of the sample-to-sample distances and progressively splitting of the dendrogram at each junction. The integrity of the resulting clusters was determined by machine learning (SVM linear).[4] Training was performed in a 10-fold randomized stratified cross validation scheme with LASSO feature selection and alpha=0.3 as implemented in the glmnet package.[5,6] When Cohens κ dropped below 0.8 no further cluster splitting was performed and thus the final cluster defined (**Supplemental Figure 2**). The LASSO genes selected for the clusters can be found in **Supplemental Tables 2-6.** This approach revealed two *BCR::ABL1* gene expression profile main cluster and four subclusters. To allow the prediction of these clusters in other cohorts, two machine learning classifiers (one for the two main clusters and one for the four subclusters) were trained using the GMALL samples and binomial logistic regression implemented in caret.[4] Regression models were used for training the final classifiers because they allow the computation of a probability score for each prediction (in contrast to deterministic SVM linear). Training was performed as described above and samples of the two main clusters and four subclusters were predicted with 92.9% and 84.1% accuracy, respectively. When not considering "Unclassified" samples the accuracies were 100% and 94.1%.

Data integration, batch correction, exon usage and differential gene expression analysis

For validation of gene expression profiles and the machine learning classifier, we used published *BCR::ABL1*-positive ALL data sets from MLL (adult, n=61)[7]St Jude n=104)[8] and PMCC (n=49)[9]. RNA-Seq datasets from GMALL, MLL, St Jude and PMCC were combined (n=327) based on 15,745 protein coding genes present in all cohorts. Batch correction was performed using the sva package[10] and TPM values were calculated. For differential gene expression analysis one-way ANOVA test was performed on log2 normalized TPMs and cutoff for significance was FDR ≤ 0.01 and absolute fold-change ≥ 2. Expression of exon usage was assessed using SGSeq Version 1.36.0.

Gene set enrichment analysis

GSEA of KEGG pathways was performed using the R package gprofiler2 with the function gost and settings ordered_query = T and multi_query = T. Analyzed were ranked gene lists of *BCR::ABL1* main and subclusters and the ranking was based on the p-values from the differential gene expression analysis and the fold change of gene expression.

Cell sorting and fluorescence in-situ hybridization (FISH)

Frozen samples (n=44) from bone marrow (n=25) or peripheral blood (n=4) at diagnosis were sorted and fixed on slides using the BD FACS Aria Fusion (BD). For n=7 patients the analysis was performed and published previously.[11] On following sorted cell populations, a *BCR*::*ABL1* FISH analysis was performed: T cells (CD45highCD19-CD3+CD16/65-), progenitor myeloid cells (M1, CD45dimCD19-CD10-CD13/33+CD34+), mature myeloid cells (M2/3, CD13/33+CD34-), malignant B cell precursors/ALL (CD45dimCD19+CD10+) and nonmalignant mature B cells (CD45highCD19+CD3-CD20+-). In case of very small M1 and M2/3 myeloid subpopulations M1 and M2/3 were sorted together as one myeloid population (M, CD45dimCD19-CD10-CD13/33+). The cell sorting strategy is depicted in the **Supplemental Figure 4.** For *BCR*::*ABL1* chromosomal fusion analysis the XL BCR/ABL1 plus translocation/dual fusion probe from MetaSystems Probes (D-5052-100-OG) was used. Samples with poor quality cells or signal were excluded from the analysis (n=10 of 44). The

signal constellation of the probe analyzed cell count and positivity for each analyzed sample (n=34) are detailed in the **Supplemental Table 12**.

Copy number analysis

Infinium Global Screening Array v3.0 arrays (Illumina) were used to assess genome wide copy number levels in n=131 patients with *BCR::ABL1*-positive BCP-ALL from samples at diagnosis of which n=102 had sufficient quality for analysis. Raw data were processed through GenomeStudio Version 2.0 (Illumina). Exported readouts were further analyzed using the Nexus BioDiscovery software (DNAnexus, Bionanao). Chromosomal alterations were assessed by logRratio and B-allele frequency profiles in Nexus and Integrative Genomics Viewer (IGV, Broad Institute). Gene related copy number variations (CNV) were analyzed using the Nexus rank segmentation approach for detection of CNV. CNV were filtered using a p-value <0.05, length of CNV >200 bases, protein coding genes only and were manually curated. All genes that had less than four CNV detected across all analyzed samples were excluded for downstream analysis. Enrichment of CNV in multilineage, lymphoid lineage or each of the four subclusters were assessed by odds ratios, Chi-square and/or Fischer's exact test. CNV for *IKZF1*, *CDKN2A*, *PAX5*, *EBF1*, *RB1* and *BTG1* were validated by multiplex-ligation probe amplification (MLPA) with the p335 Kit from MRC Holland, as described previously.[12,13] The distribution of recurrent genetic alterations was visualized using the cBioPortal OncoPrinter.[14]

Whole genome sequencing

Whole genome sequencing was analyzed as previously described.[7] For CNV analysis a mean log2 copy ratio cut of >0.2 for amplifications and <-0.2 for deletions was used. The discrimination into heterozygous and homozygous deletions was not done using WGS. *IKZF1* deletions were validated by PCR and *CDKN2A* deletions by FISH.

Extraction of poly(A)-enriched RNA for nanopore direct RNA sequencing

Poly(A)-enriched mRNA was isolated from frozen bone marrow samples by using the Dynabeads mRNA DIRECT purification kit (Thermo Fisher Scientific, 61011) according to manufacturer's instructions with minor modifications. Briefly frozen bone marrow samples were

thawed on ice and transferred into a fresh 1,5 ml DNA LoBind tube (Eppendorf, 0030108051) with subsequent centrifugation for 3 min and 500 xg at 4°C. The supernatant was completely removed and the cell pellet was carefully resuspended in 1.25 ml Lysis/Binding buffer. To reduce the sample viscosity caused by released genomic DNA, the lysates were passed through a 21-gauge needle (Becton Dickinson, 304432) five times and then added to the prewashed Oligo(dT)25 beads. The beads/mRNA complex was hybridized on a Mini Rotator PTR-25 (Grant-bio) for 10 min and the tubes were placed on a DynaMag2 magnet (Thermo Fisher Scientific, 12321D) until the beads were completely immobilized. DNA-containing supernatant was discarded and beads were resuspended twice with 2 ml buffer A, followed by a second wash step with 2×1 ml buffer B. Purified RNA was eluted with 10 µL preheated elution buffer (10 mM Tris-HCl pH 7.5) for 5 min at 80°C and quantified with a Qubit Fluorometer (Thermo Fisher Scientific) using the RNA HS Assay Kit (Thermo Fisher Scientific, Q32852). The eluted RNA samples were used immediately for the preparation of nanopore direct RNA sequencing libraries.

Preparation of Nanopore Direct RNA Sequencing Libraries

RNA sequencing libraries were prepared according to the manufacturer's instructions (ONT, SQK-RNA002) with minor modifications. Briefly, 600 ng of freshly prepared poly(A)-enriched mRNA was used for the primer annealing and ligation reaction. The RNA calibrant strand was omitted. Samples obtained from the reverse transcription reaction were bound to 72 µl of Agencourt CleanXP beads and subsequently washed with 80% ethanol solution. The final library was loaded onto R9.4.1 MinION flow cells (ONT, FLO-MIN106) and sequenced for 72 h by using ONT's MinKNOW software (v20.10.3). The resulting raw read data were basecalled by taking advantage of guppy (v6.4.6) using the rna_r9.4.1_70bps_hac model. Base-called reads were aligned to the human reference genome hg38 using minimap2 (v2.24) with the Oxford Nanopore Technologies parameter preset for spliced alignments (-ax splice -uf -k14) and the resulting BAM files were visualized using the Integrative Genomic Viewer (IGV, v2,16).

scATAC-Seq and scRNA-Seq

Single cell ATAC combined with single-cell (sc) RNA sequencing (10x Genomics, Pleasanton, USA) were used to confirm cluster-specific gene isoform expression. *BCR::ABL1*-positive samples representing different diseases i.e. two del7 ALL, one IKZF1 ALL, one AML and one CML blast phase. Frozen mononuclear cells from peripheral blood or bone marrow samples were thawed and enriched for live cells using the Dead Cell Removal Kit (Miltenyi Biotec) according to the manufacturer's instructions. Cell count and viability were assessed with AOPI staining using a Luna-FX7 automated cell counter. Nuclei were isolated following the Nuclei Isolation for Single Cell Multiome ATAC and Gene Expression Sequencing User Guide (CG000365 Rev C). GEM generation and single cell libraries were prepared according to the Chromium Next GEM Single Cell Multiome ATAC and Gene Expression User Guide (CG000338 Rev F). Libraries were sequenced on the Illumina NovaSeq according to 10X Genomics setting. FASTQ generation, alignment (reference GRCh38-2020-A-2.0.0), filtering, barcode counting, peak calling, and counting of both ATAC and GEX molecules was performed using cellranger-arc (version 2.0.2). Comparison of peak-calling and gene expression analysis was performed using Signac (1.11.9000)[15] and Seurat (4.9.9.9060)[16]. For scATAC-Seq term frequency inverse document frequency (TF-IDF) normalization was performed, followed by singular value decomposition and UMAP dimension reduction. Final cell types were assigned by marker gene expression.

Statistical analyses

Relationships between individual analyses and the defined *BCR*::*ABL1* expression clusters (multilineage vs lymphoid lineage or delHBS1L vs del7 vs IKZF1 vs CDKN2A/PAX5) were assessed by Chi-square or Fischer's Exact test for categorical variables and by Mann-Whitney-U, Kruskal-Wallis test or one-way ANOVA for continuous variables. All statistical calculations were performed using R version 4.1.0, SPSS statistics (IBM) version 27 and SciPy (version 1.7.1).

References

1. Pfeifer H, Raum K, Markovic S, et al. Genomic CDKN2A/2B deletions in adult Ph+ ALL are adverse despite allogeneic stem cell transplantation. *Blood*. 2018;131(13):1464–1475.

2. McInnes L, Healy J, Melville J. UMAP: Uniform Manifold Approximation and Projection for Dimension Reduction. 2020;

3. Källberg D, Vidman L, Rydén P. Comparison of Methods for Feature Selection in Clustering of High-Dimensional RNA-Sequencing Data to Identify Cancer Subtypes. *Front. Genet.* 2021;12:632620.

4. Kuhn M. Building Predictive Models in *R* Using the **caret** Package. *J. Stat. Softw.* 2008;28(5):.

5. Tibshirani R. THE LASSO METHOD FOR VARIABLE SELECTION IN THE COX MODEL. *Stat. Med.* 1997;16(4):385–395.

6. Friedman J, Hastie T, Tibshirani R. Regularization Paths for Generalized Linear Models via Coordinate Descent. *J. Stat. Softw.* 2010;33(1):1–22.

7. Walter W, Shahswar R, Stengel A, et al. Clinical application of whole transcriptome sequencing for the classification of patients with acute lymphoblastic leukemia. *BMC Cancer*. 2021;21(1):886.

8. Gu Z, Churchman ML, Roberts KG, et al. PAX5-driven subtypes of B-progenitor acute lymphoblastic leukemia. *Nat. Genet.* 2019;51(2):296–307.

9. Kim JC, Chan-Seng-Yue M, Ge S, et al. Transcriptomic classes of BCR-ABL1 lymphoblastic leukemia. *Nat. Genet.* 2023;55(7):1186–1197.

10. Leek JT, Johnson WE, Parker HS, Jaffe AE, Storey JD. The sva package for removing batch effects and other unwanted variation in high-throughput experiments. *Bioinformatics*. 2012;28(6):882–883.

11. Beder T, Hansen B-T, Hartmann AM, et al. The gene expression classifier ALLCatchR identifies B-precursor ALL subtypes and underlying developmental trajectories across age. Cancer Biology; 2023.

12. Bastian L, Schroeder MP, Eckert C, et al. PAX5 biallelic genomic alterations define a novel subgroup of B-cell precursor acute lymphoblastic leukemia. *Leukemia*. 2019;33(8):1895–1909.

13. Krentz S, Hof J, Mendioroz A, et al. Prognostic value of genetic alterations in children with first bone marrow relapse of childhood B-cell precursor acute lymphoblastic leukemia. *Leukemia*. 2013;27(2):295–304.

14. Cerami E, Gao J, Dogrusoz U, et al. The cBio Cancer Genomics Portal: An Open Platform for Exploring Multidimensional Cancer Genomics Data. *Cancer Discov.* 2012;2(5):401–404.

15. Stuart T, Srivastava A, Madad S, Lareau CA, Satija R. Single-cell chromatin state analysis with Signac. *Nat. Methods*. 2021;18(11):1333–1341.

16. Hao Y, Stuart T, Kowalski MH, et al. Dictionary learning for integrative, multimodal and scalable single-cell analysis. *Nat. Biotechnol.* 2023;

Supplemental Figure 1

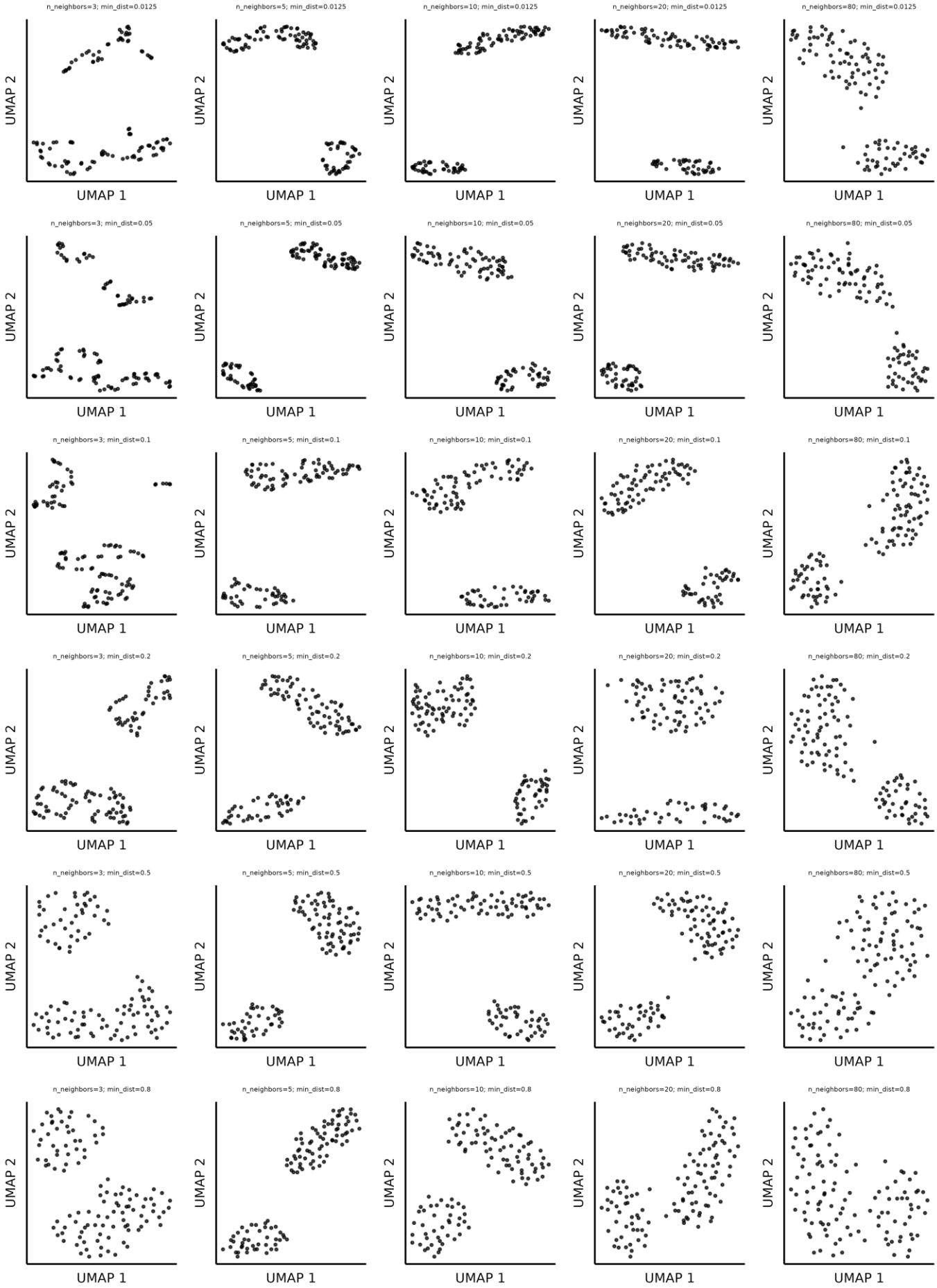

Supplemental Figure 1. Influence of UMAP parameters on grouping of *BCR::ABL1*-positive ALL samples. *BCR::ABL1*-positive ALL GMALL samples (n=113) are grouped using UMAP and are based on 200 genes with lowest p-value in Hartigans' dip test for multimodality. The 30 different UMAP parameter combinations for n_neighbors and min_dist are shown that were used to calculate the average sample-to-sample distance (**Main Figure 1B**).

Supplemental Figure 2

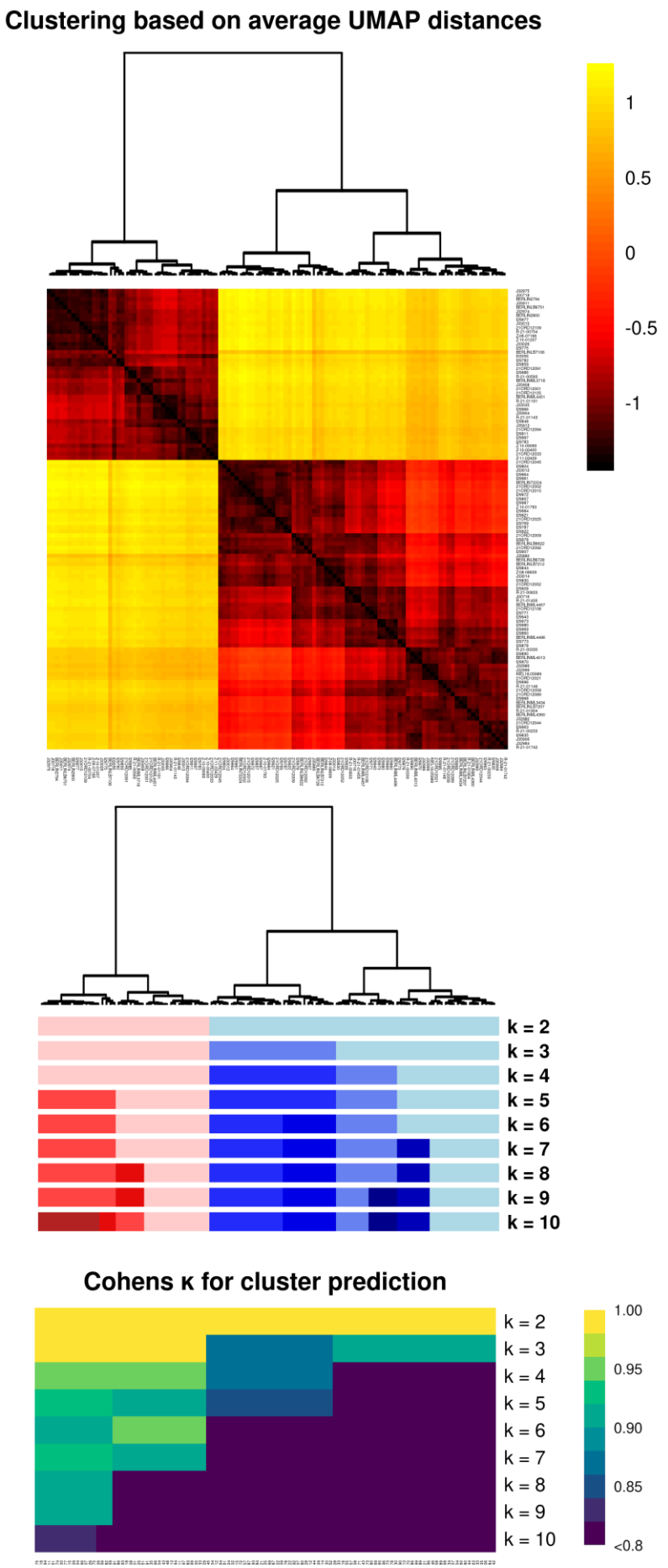

Supplemental Figure 2. Clustering of averaged UMAP distances and testing of cluster integrity by machine learning. *BCR::ABL1*-positive GMALL samples (n=113) form distinct clusters based on the average UMAP sample-to-sample distances in the heatmap (upper panel). The dendrogram was progressively split along the junctions forming 2-10 clusters (middle panel). Machine learning (SVM linear) was applied to test the predictability of samples within the clusters. When the predictability of a cluster as determined by Cohens κ dropped below 0.8 no further cluster splitting was performed and thus the final cluster defined (lower panel).

Supplemental Figure 3

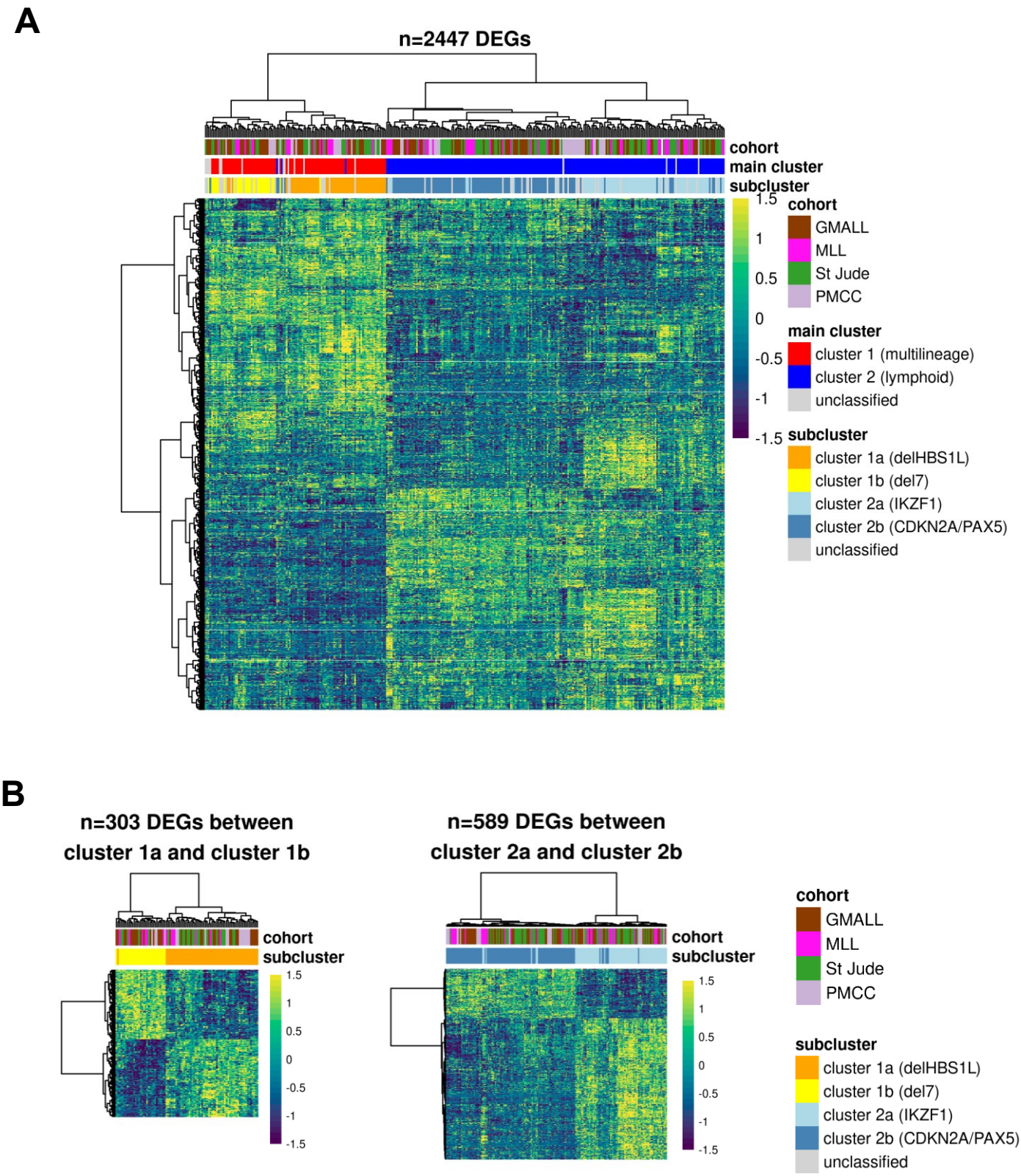

Supplemental Figure 3. Differentially expressed genes between the 4 subclusters in the integrated dataset. (**A**) Hierarchical clustering of 2447 differentially expressed genes between the 4 subclusters (one-way ANOVA test, fold-change ≥ 2 / FDR: ≤ 0.01). The corresponding gene sets are included in Supplemental Tables 8-11. (**B**) Differentially expressed genes between multilineage and lymphoid lineage subcluster samples. Heatmaps showing batch corrected z-scores of tpms.

Supplemental Figure 4

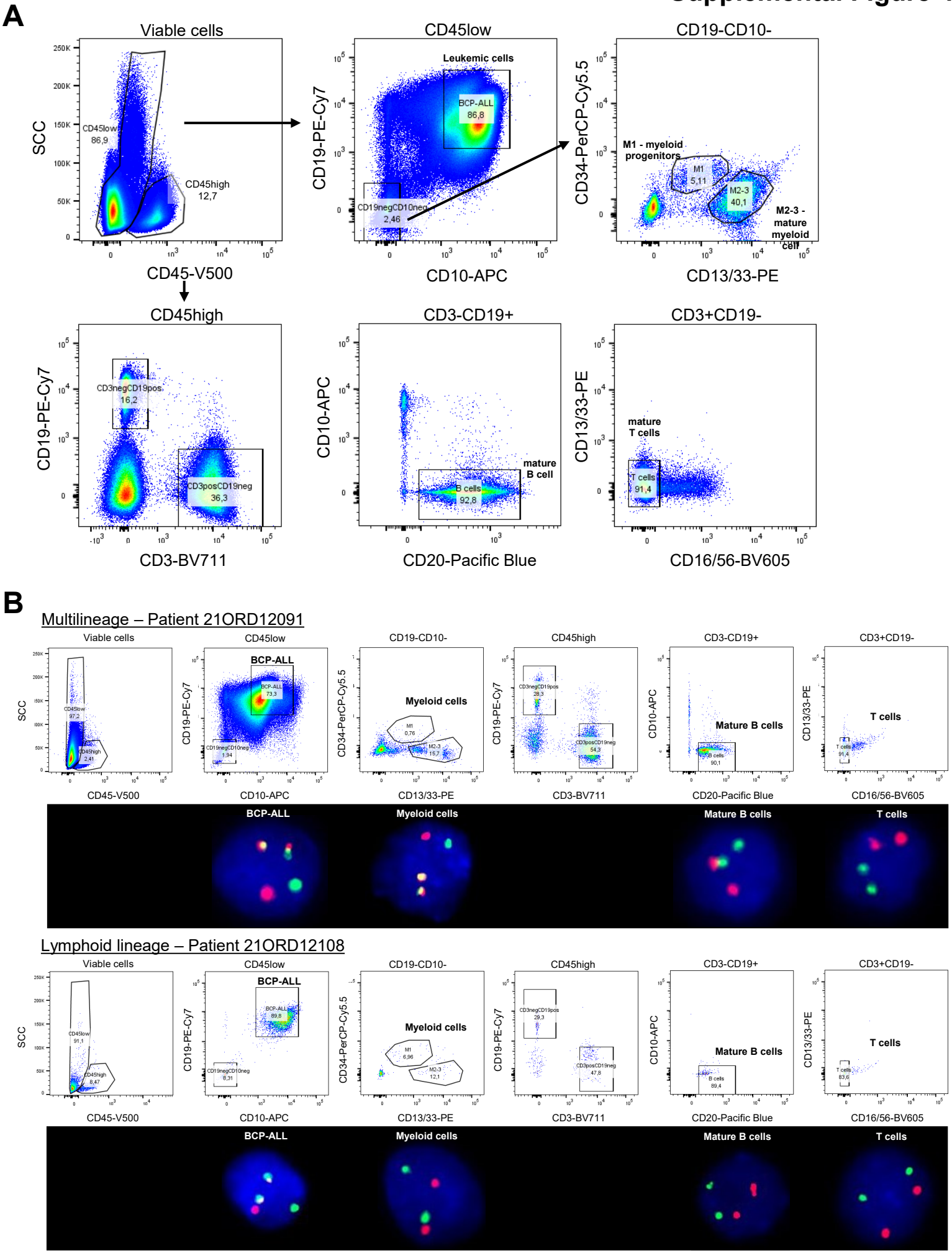

Supplemental Figure 4. Sorting strategy for hematopoietic cell compartments and BCP-ALL for subsequent *BCR::ABL1* FISH analysis. (**A**) Flow cytometry scheme used to sort mature B cells, T cells, precursor myeloid cells (M1 and M2/3) and B cell precursor cells from human frozen bone marrow or peripheral blood at primary diagnosis of BCP-ALL. (**B**) Representative images of *BCR::ABL1* FISH of FACS sorted cells shown for one mutlilineage and one lmphoid lineage *BCR::ABL1*-positive ALL case.

A

	multilineage		lymphoid lineage		p-value	p-value
	het del (%)	hom del (%)	het del (%)	hom del (%)	het del	hom del
Chromsome 6q	0	0	3	0	0.551	NA
HBS1L	43.8	0	3	0	**<0.001**	NA
MYB	0	0	3	0	0.551	NA
MEF2C	14.6	0	3	0	**0.013**	NA
monosomy 7	35.4	0	5	0	**<0.001**	NA
IKZF1	72.9	4.2	64.4	11.9	0.353	0.228
Chromsome 9p	0	0	29.7	0	**<0.001**	NA
PAX5	8.3	0	50.5	0	**<0.001**	NA
CDKN2A/B	0	4.2	29.7	21.8	**<0.001**	**0.007**
EBF1	10.4	0	8.9	0	0.770	NA
RB1	4.2	2.1	10.9	3	0.225	1.000
BTG1	8.3	0	22.8	5	**0.040**	0.176
SLX4IP	4.2	0	16.8	0	**0.035**	NA
VPREB1	12.5	2.1	35.6	4	**0.003**	1.000
High hyperdiploid	0		17.8		**0.002**	

B

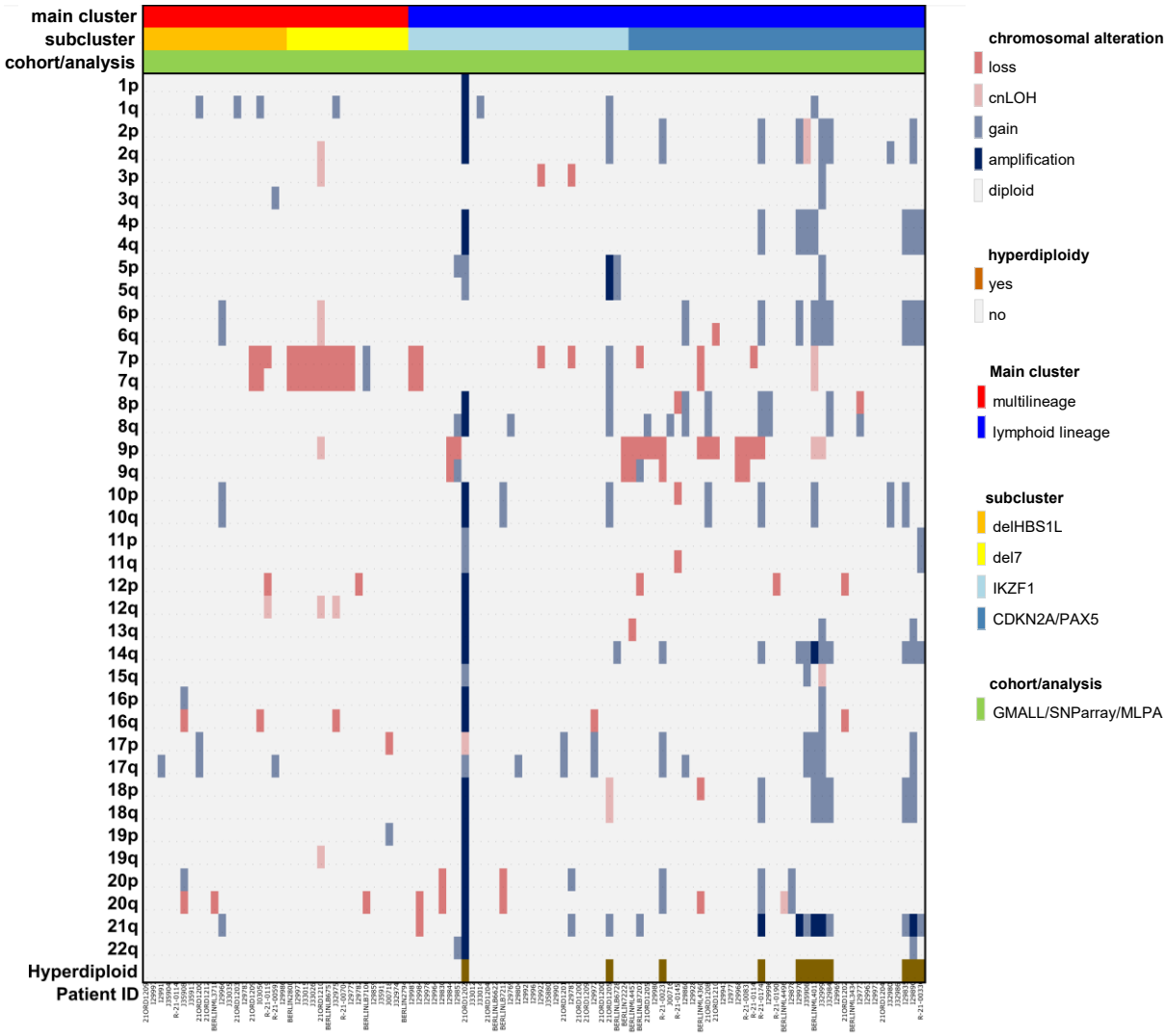

Supplemental Figure 5. Association of distinct gene expression clusters with recurrent genetic alterations in *BCR::ABL1*-positive BCP-ALL. (**A**) Distribution of recurrent genetic alterations in *BCR::ABL1*-positive samples defined as multilineage (n=48) or lymphoid (n=101) lineage B cell precursor (BCP) ALL. Bars represent the percentage of cases with a given genetic alteration within each category. P-values below 0.05 are depicted in bold. (**B**) Distribution of chromosomal gains and losses. Virtual karyotypes were assessed by SNParray. Colored bars represent a copy number alteration at diagnosis of ALL.

Supplemental Figure 6

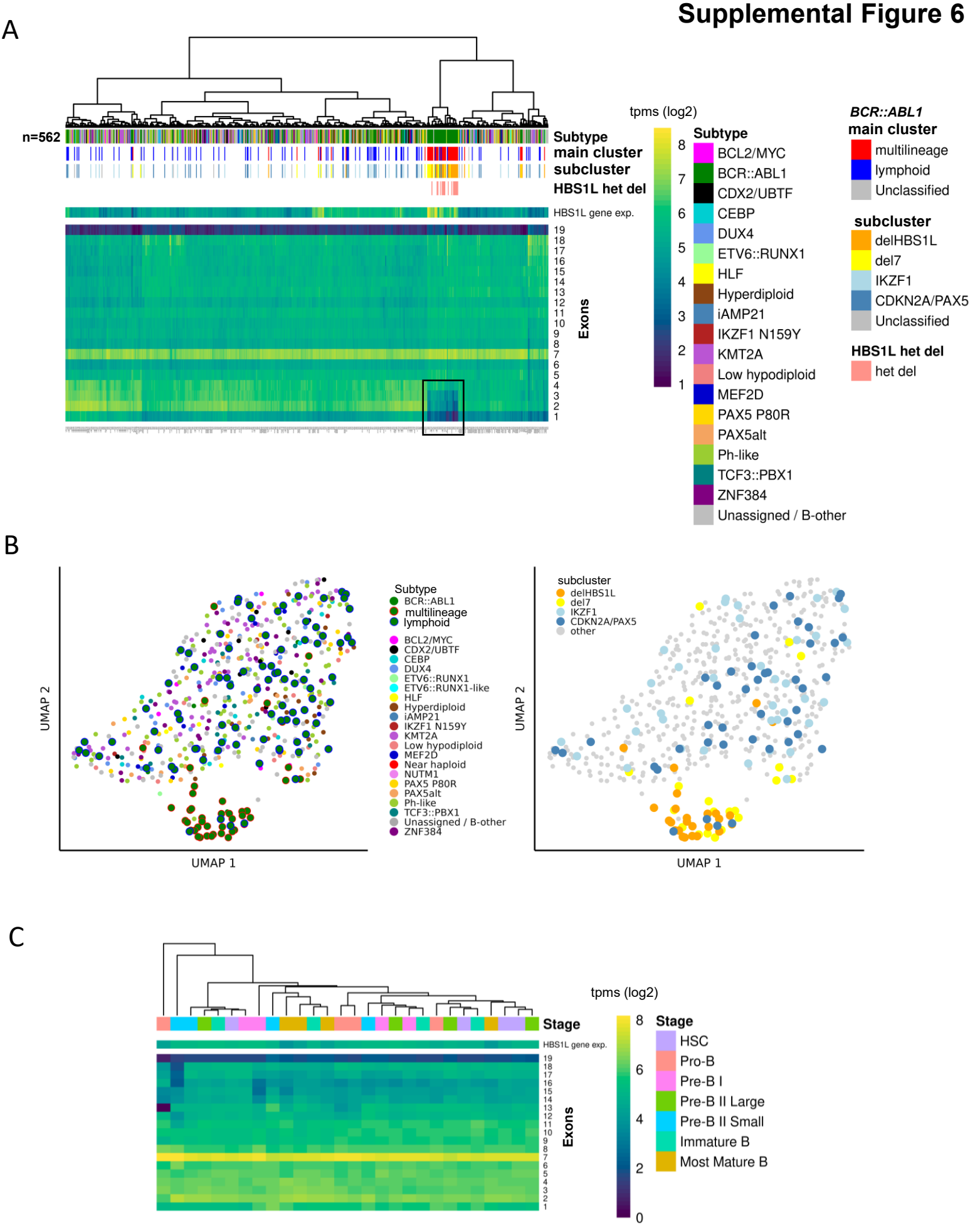

Supplemental Figure 6. *BCR::ABL1*-positive ALL samples from multilineage main cluster have an increased *HBS1L* gene expression and an altered exon usage. (**A**) *BCR::ABL1* multilineage samples group together by hierarchical clustering based on the *HBS1L* gene and exon expression and have a reduced coverage of exons 1-3. Interestingly, *BCR::ABL1* del7 samples show the same aberration as samples with HBS1L deletions (delHBS1L). (**B**) UMAP analysis based on HBS1L gene expression and exon coverage. (**C**) In healthy B cell progenitors no altered *HBS1L* exon 1-3 coverage was observed.

Supplemental Figure 7

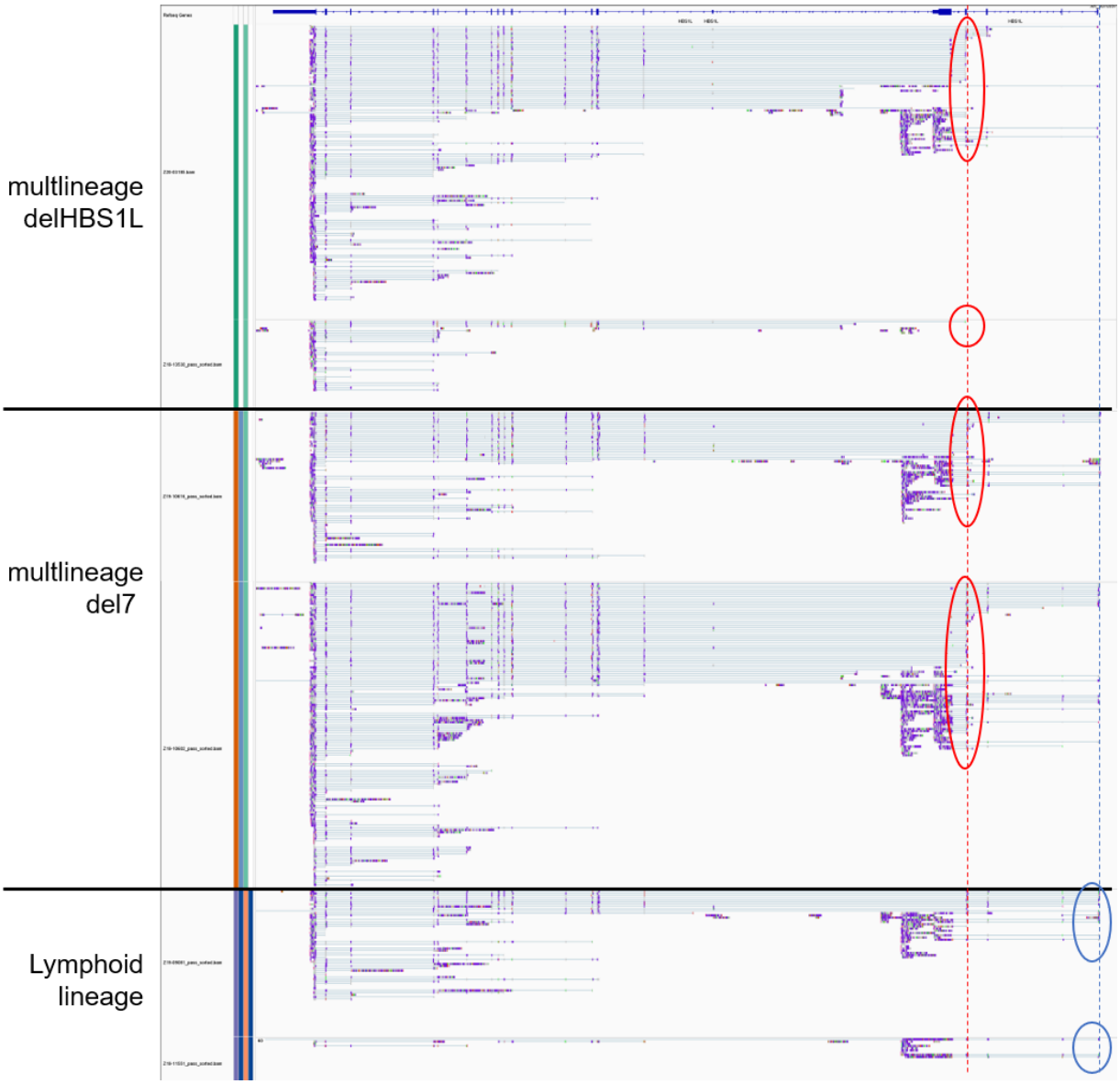

Supplemental Figure 7. Long-read RNA sequencing identifies novel *HBS1L* isoform and alternative transcription start side in multilineage samples independent of the *HBS1L* deletion. (**A**) Long-read direct RNA sequencing of n=2 delHBS1L, n=2 del7 and n=2 lymphoid cases. Red circles indicate the start of the alternative *HBS1L* isoform in exon 4. Blue circles show the start of the canonical *HBS1L* isoform ENST00000367837 in exon 1. Sequencing data are shown as displayed in the integrative genomic viewer (IGV). (**B**) Long-read sequencing reads are shown for one delHBS1L and one lymphoid case with coverage as displayed in the IGV for the region of the depicted alternative promoter (red box, line and arrow) and exon 4 (chr6:135,039,570-135,040,447). In blue are the canonical transcripts, in orange the translated transcript, in brown the transcribed transcript inferred from the reads using BLAT. (**C**) Expression from short read sequencing from n=493 GMALL samples at the alternative transcription start side chr6:135,040,344-135,040,447 (GRCh38hg38), indicated by black lines. The red line indicates the alternative promoter.

Supplemental Figure 8

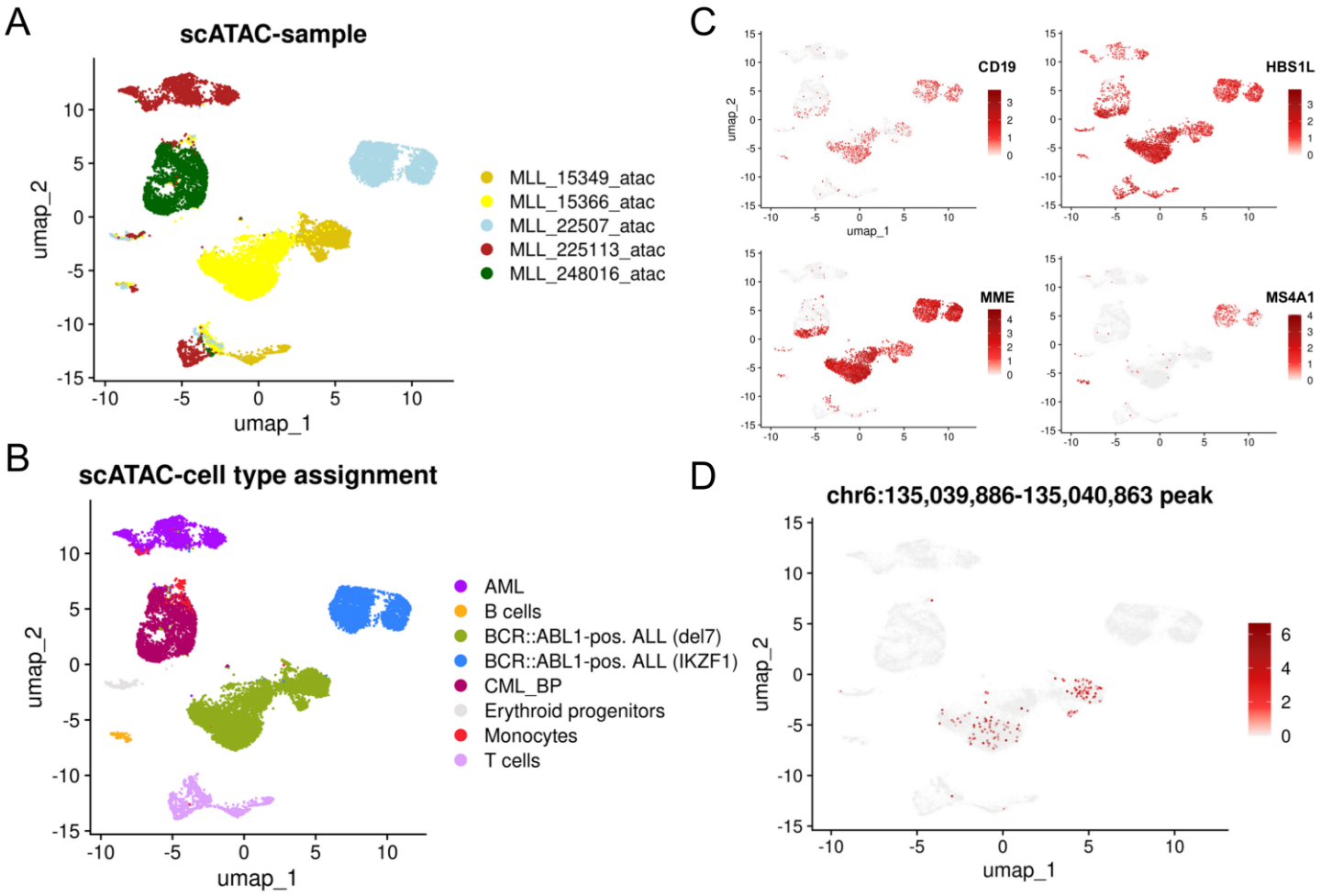

Supplemental Figure 8. Single cell ATAC-Seq combined with scRNA-Seq reveals open chromatin peak at the alternative promoter of *HBS1L*alt in multilineage samples lacking the HBS1L deletion. (**A**) UMAP plot showing *BCR::ABL1*-positive samples representing different diseases i.e. two del7 ALL (MLL_15349 and MLL_15366), one IKZF1 ALL (MLL_22507), one AML (MLL_225113) and one CML blast phase (MLL_248016). Samples were analyzed using scATAC-Seq combined with scRNA-Seq and UMAP analysis was based on scATAC-Seq data. (**B**) Cell types were defined by marker gene expression. (**C**) Expression of marker genes from scRNA-Seq projected on the scATAC-Seq UMAP illustrate general B-cell marker gene expression (CD19 and MME) in both del7 and the IKZF1 ALL samples, but the mature B-cell marker *MS4A1* is expressed predominantly in the IKZF1 ALL. *HBS1L* expression was observed across all cell types. (**D**) A peak, called from scATAC-Seq, which overlaps with the *HBS1L*alt transcription start site was exclusively present in del7 ALL samples, indicating regulatory mechanisms leading to the expression of the alternative HBS1L transcript in multilineage samples, even in the absence of the HBS1L deletion.

Supplemental Figure 9

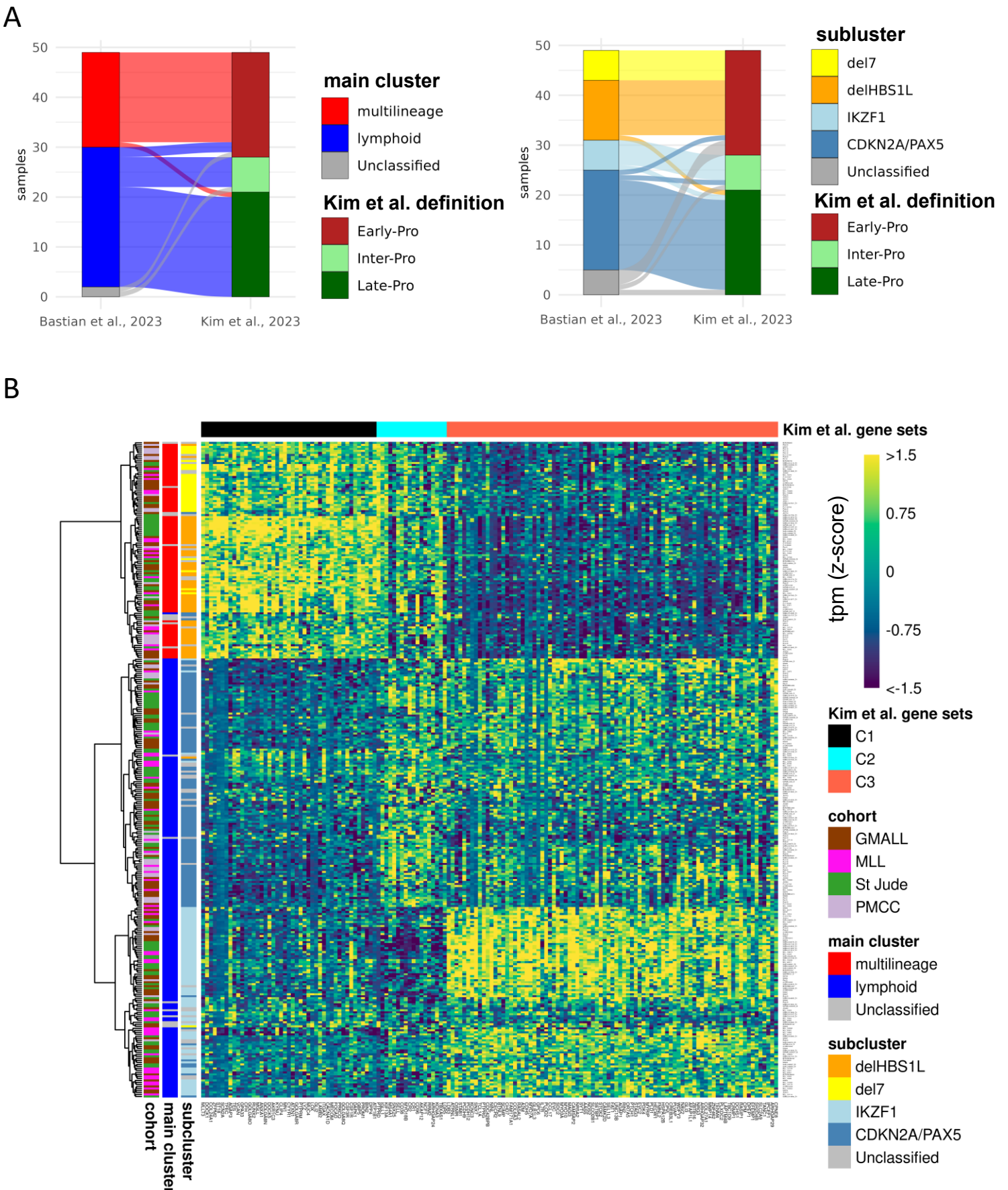

Supplemental Figure 9. Extension of *BCR::ABL1* cluster definitions by Kim *et al.* Recently Kim JC *et al.*[14] (PMCC cohort) defined three distinct gene expression clusters in *BCR::ABL1*-positive ALL patients. The four subcluster in the present study extend these definitions. (**A**) Sankey plots showing representation of the main and subcluster prediction to Kim JC *et al.* definitions. (**B**) Genes sets defining C1 (Early-Pro), C2 (Inter-Pro) and C3 (Late-Pro) were used for grouping samples from the integrated dataset. Samples group into multilineage and lymphoid main clusters and additionally the separation in the four subclusters characterized by delHBS1L, monosomy 7 as well IKZF1 and CDKN2A/PAX5 copy number alterations can be seen.

Supplemental Figure 10

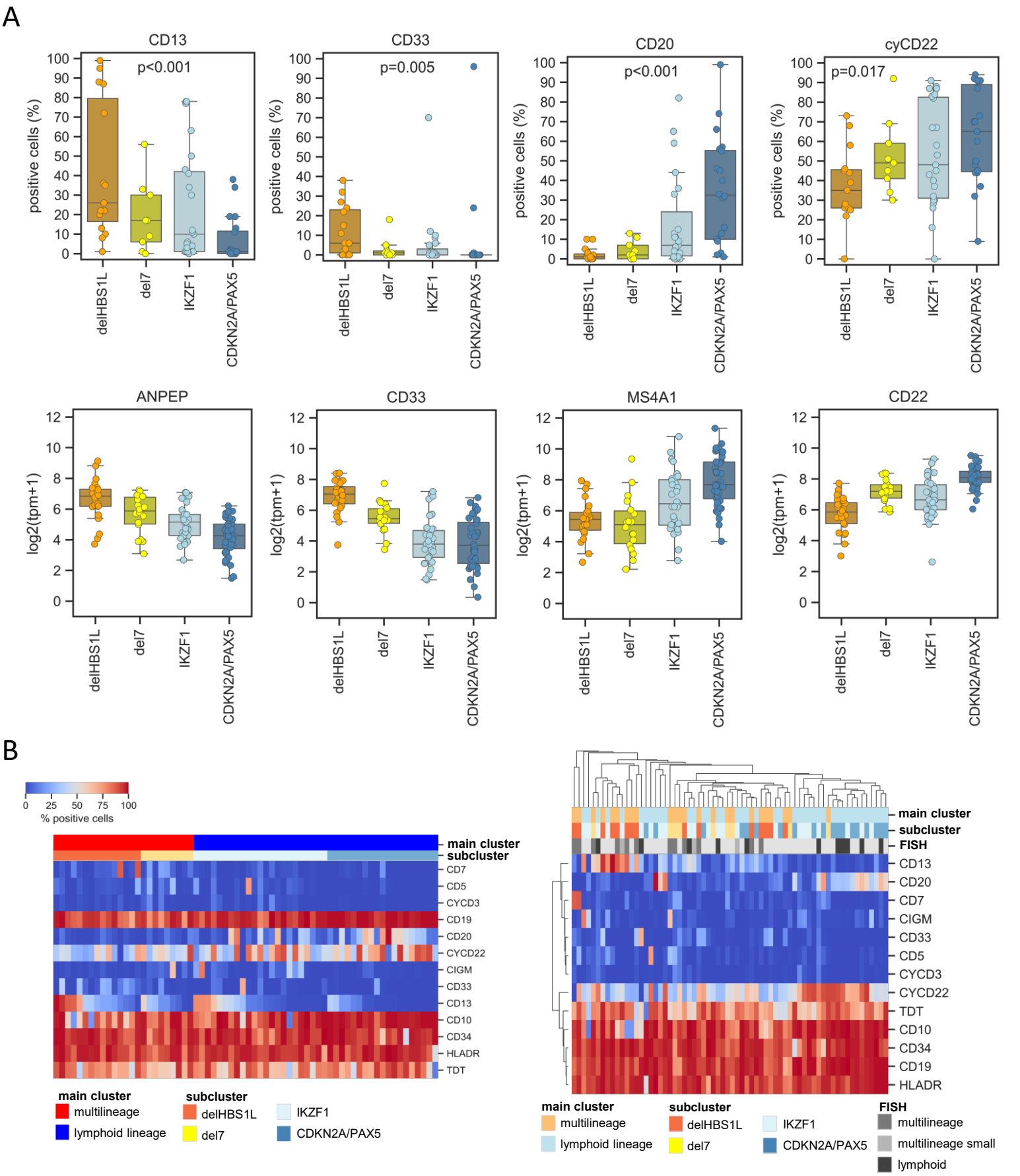

Supplemental Figure 10. Myeloid surface marker are co-expressed in multilineage *BCR::ABL1*-positive ALL cases. (**A**) Expression of surface markers from flow cytometry analysis (upper panel) or RNA sequencing (lower panel) for each subcluster are shown as boxplots. (**B**) Ordered heatmap (left panel) and clustered heatmap (right panel) showing the expression of surface markers measured by flow cytometry at diagnosis for n=66 patients with *BCR::ABL1*-positive ALL.

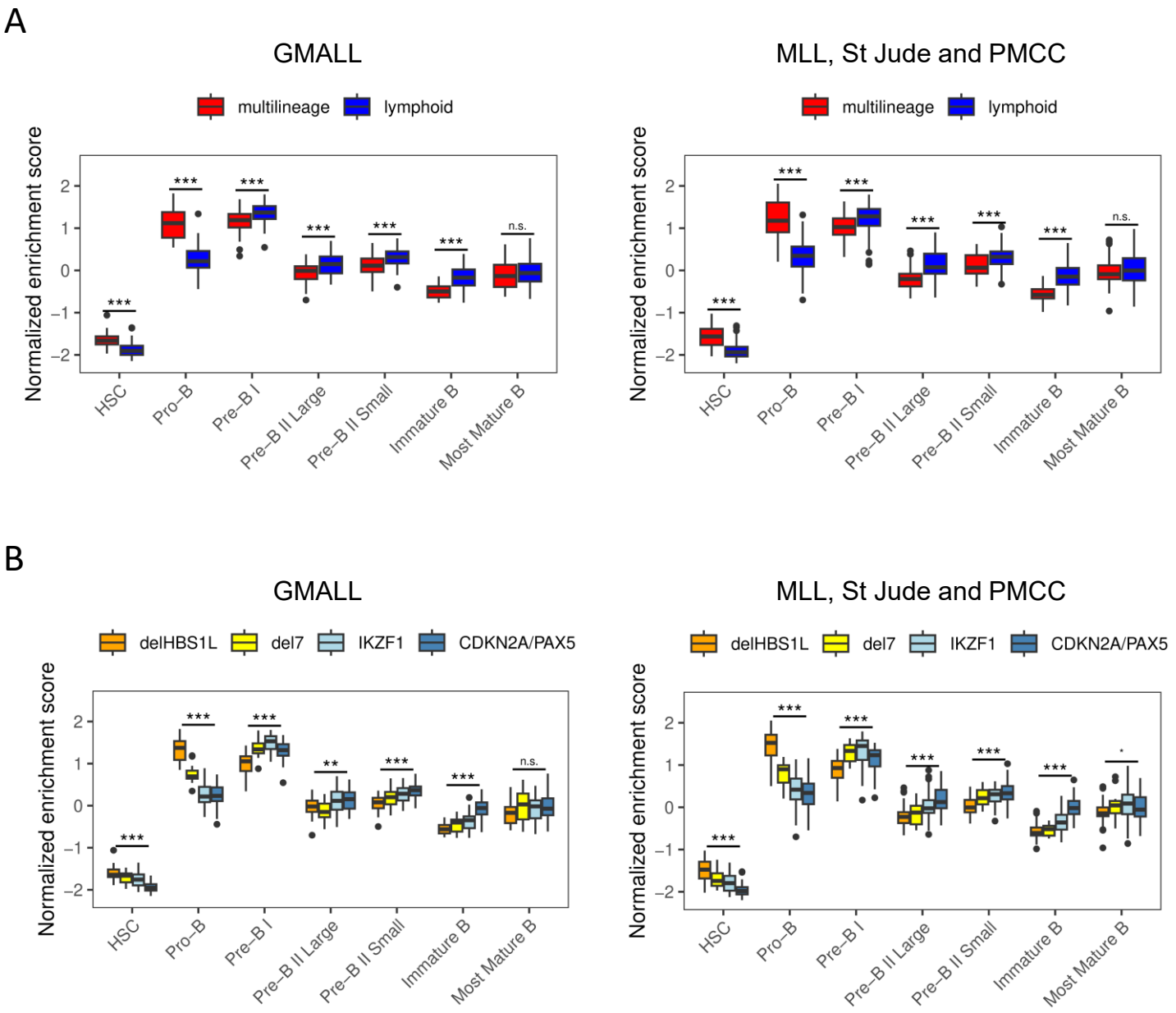

Supplemental Figure 11. Enrichment scores of *BCR::ABL1*-positive ALL samples to gene sets defined for seven B cell differentiation stages. Enrichment scores of ALLCatchR for samples from the two lineage driven main clusters (**A**) and the four subclusters (**B**) to gene sets defined for seven B cell differentiation stages are shown. Data for GMALL (the discovery cohort) and testing cohorts (MLL, St Jude and PMCC) are shown. Largest differences were observed in pro-B indicating a higher resemblance of multilineage samples (especially delHBS1L) to earlier differentiation stages. In contrast lymphoid samples were more similar to later differentiation stages.

A

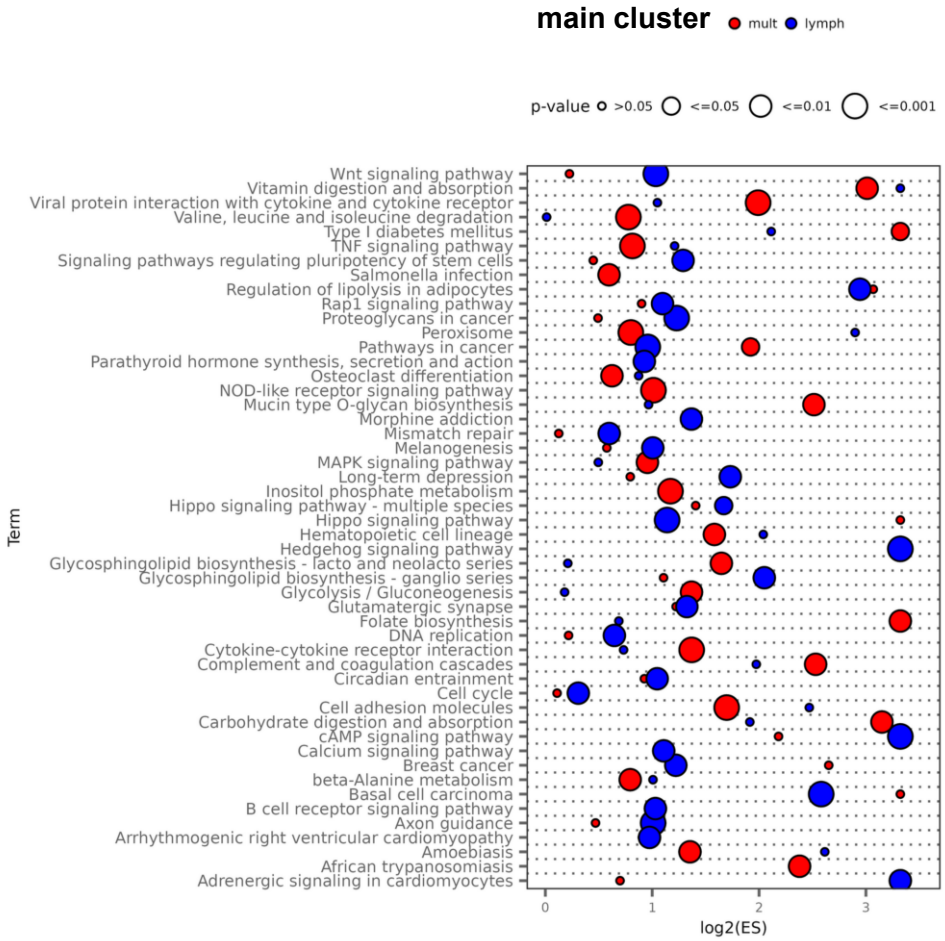

B

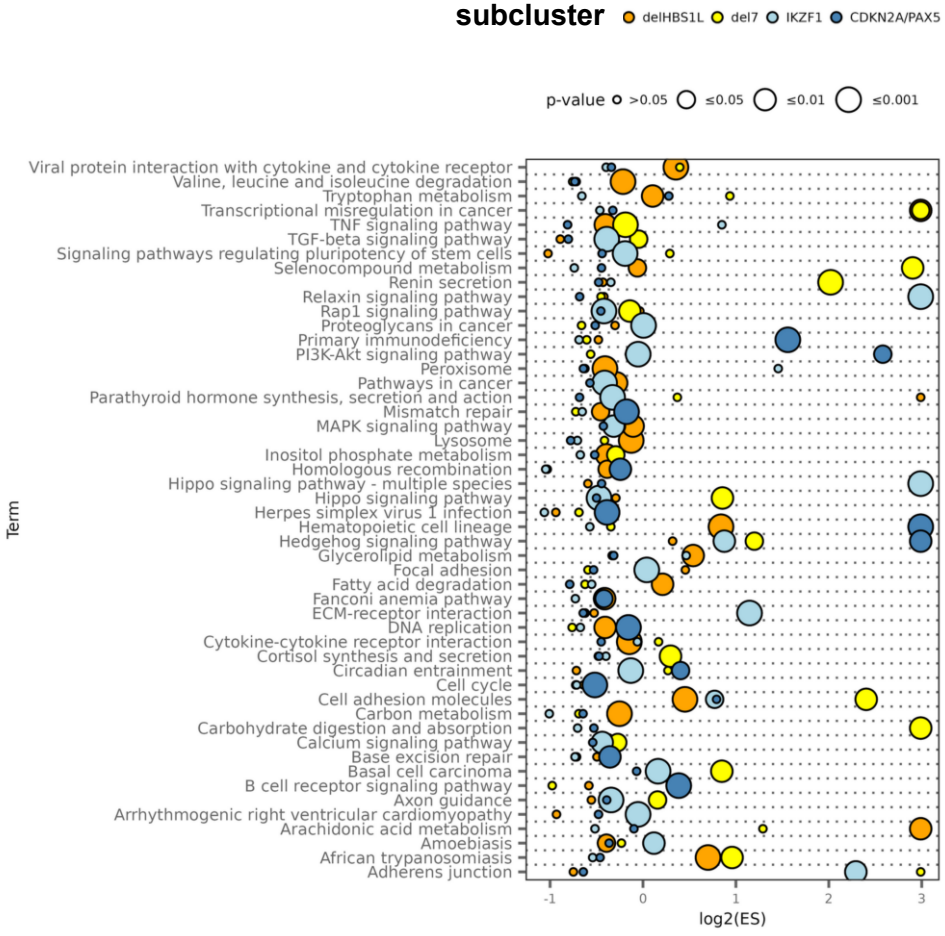

Supplemental Figure 12. Gene set enrichment analysis of main and subclusters. Gene set enrichment analysis was performed using gprofiler and was based on the ranking of genes in the differential gene expression analysis of main cluster **(A)** and subcluster (**B**) samples**.** Top 50 enriched KEGG pathways are shown.

Supplemental Figure 13

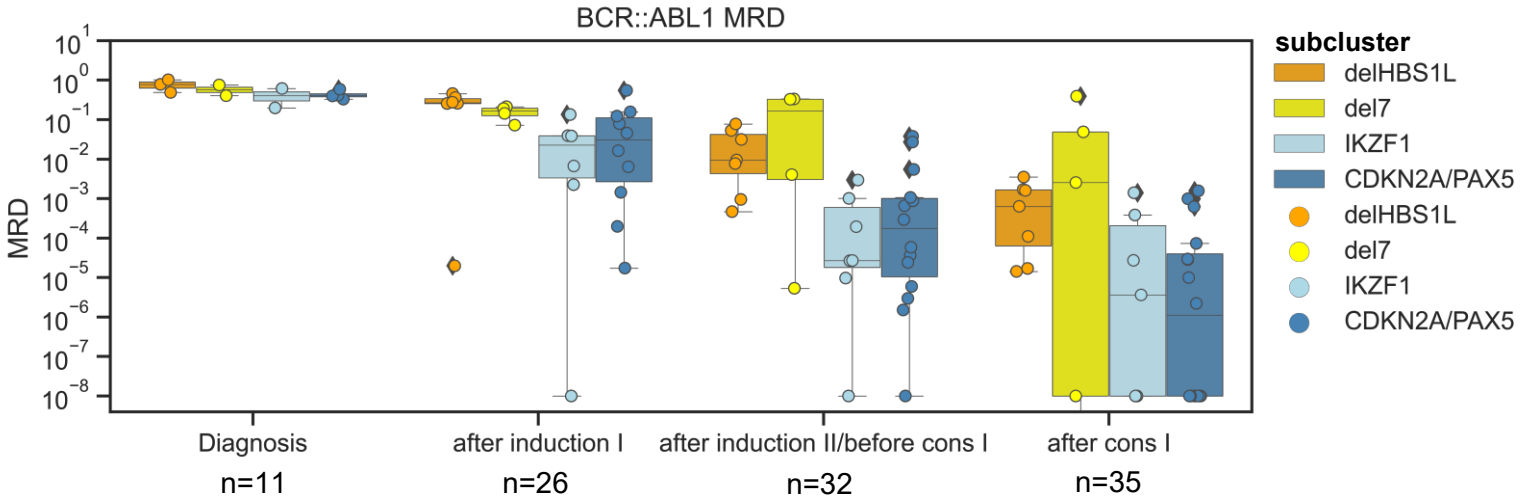

Supplemental Figure 13. Defined *BCR*::*ABL1* subtypes present with different MRD levels during the course of treatment. Minimal residual disease (MRD) plot for *BCR::ABL1* transcript levels for each subtype at different time points during treatment. Each dot represents a patient with a MRD measurement at the defined time point.